OPEN ACCESS
IOP PUBLISHING
SCIENCE AND TECHNOLOGY OF ADVANCED MATERIALS
Sci. Technol. Adv. Mater. **14** (2013) 065004 (8pp)
doi:10.1088/1468-6996/14/6/065004

Concurrent zero-dimensional and one-dimensional biomineralization of gold from a solution of Au^{3+} and bovine serum albumin

Matthew R Hartings[1], Noah Benjamin[1], Floriene Briere[1], Maria Briscione[1], Omar Choudary[1], Tamra L Fisher[1], Laura Flynn[1], Elizabeth Ghias[1], Michaela Harper[1], Nader Khamis[1], Catherine Koenigsknecht[1], Klare Lazor[1], Steven Moss[1], Elaine Robbins[1], Susan Schultz[1], Samiye Yaman[1], Luke M Haverhals[2,4], Paul C Trulove[2], Hugh C De Long[3], Abigail E Miller[1] and Douglas M Fox[1]

[1] Department of Chemistry, American University, 4400 Massachusetts Avenue, NW, Washington, DC 20016, USA
[2] Department of Chemistry, US Naval Academy, Anapolis, MD 21402, USA
[3] Directorate of Math, Information, and Life Sciences, US Air Force Office of Scientific Research, Arlington, VA 22203, USA

E-mail: hartings@american.edu

Received 19 April 2013
Accepted for publication 28 October 2013
Published 20 November 2013
Online at stacks.iop.org/STAM/14/065004

Abstract
A technique was developed for preparing a novel material that consists of gold nanoparticles trapped within a fiber of unfolded proteins. These fibers are made in an aqueous solution that contains $HAuCl_4$ and the protein, bovine serum albumin (BSA). By changing the ratio of gold to BSA in solution, two different types of outcomes are observed. At lower gold to BSA ratios (30–120), a purple solution results after heating the mixture at 80 °C for 4 h. At higher gold to BSA ratios (130–170), a clear solution containing purple fibers results after heating the mixture at 80 °C for 4 h. UV–Vis spectroscopy and light scattering techniques show growth in nanocolloid size as gold to BSA ratio rises above 100. Data indicate that, for the higher gold to BSA ratios, the gold is sequestered within the solid material. The material mass, visible by eye, appears to be an aggregation of smaller individual fibers. Scanning electron microscopy and transmission electron microscopy indicate that these fibers are primarily one-dimensional aggregates, which can display some branching, and can be as narrow as 400 nm in size. The likely mechanism for the synthesis of the novel material is discussed.

Keywords: biomineralization, gold nanoparticle, protein aggregation, protein-templated nanoparticle, peptide-templated nanoparticle

S Online supplementary data available from stacks.iop.org/STAM/14/065004/mmedia

[4] Current address: Mund-Lagowski Department of Chemistry and Biochemistry, Bradley University, Peoria, IL 61625, USA.

1. Introduction

The ability of proteins and peptides to template and structure inorganic materials occurs in many species across nature; bones, teeth, shells, diatom frustules and coral exoskeletons are all examples of these types of substances [1–3]. In the process of biomineralization, proteins play a major role in dictating the morphology of crystal packing of the inorganic material at the nanometer scale. Shaping at this small scale then translates to bulk properties that we can observe by eye. In order to create new bioinorganic materials with defined chemical and physical properties for potential applications in biotechnology, these examples show that proteins can play a significant role in dictating what these properties are.

Biocompatible nanoparticles (NPs) account for one of the major technologies at the forefront of new biotechnological applications [4–12]. Colloidal NPs and semiconductor quantum dots are being investigated for their potential applications in diagnostics, therapeutics, fluorescence imaging, magnetic resonance imaging and drug delivery, among others. For most of these cases, the NPs are stabilized by small molecules, such as citrate, alkanethiols or polar lipids [13–15]. The NPs are then further modified with specific biomolecules (antibodies, DNA, etc) in order to direct their function. Conventional wisdom has been that the best way to control the chemical and physical properties of these materials is through interactions with small-molecule stabilizers. However, if used properly, proteins alone can and do template NP synthesis and, further, stabilize the NPs in solution [16].

At the crystal packing scale, a consensus is beginning to emerge about the sequence requirements needed for NP synthesis [2, 17–25]. When examining the reactions that must occur, the following are basic to the formation of metal NPs: (i) the reagents most often include a charged metal salt; (ii) the metal ion must be reduced to its elemental form; (iii) the metal atom needs to interact with a ligand in order to keep it suspended within the reaction solvent; and (iv) the ligands must organize the structure of the growing metal colloid. For proteins to be able to template NP growth, it is not surprising that a protein needs to be able to reduce a metal ion and have a strong metal binding affinity. For proteins, the tryptophan (W) residues, tyrosine (Y) residues and disulfide bonds (from cysteine residues) are the most likely sources of reducing electrons. There are several amino acids that can contribute different levels of binding affinity to the reduced metal through both their side chains and backbone atoms. It was recently found, though, that a delicate balance between reducing strength and binding strength needed to be considered when designing polypeptides that are efficient at producing NPs [20, 21]. A separate study described how protein phage displays could creatively be used to find polypeptide sequences that show affinity for very specific types of crystal lattices [19]. Individual peptides were then synthesized to match these sequences, and the peptides were able to template precisely the NP shape whose lattice structure matched the peptide's binding profile.

With many large proteins, some of the nuance is lost in comparison with the peptide templating studies, but full proteins are certainly capable of enabling NP synthesis [2, 13, 26–36].

Perhaps the most prominent example of this is ferritin [29, 37, 38]. Ferritin is a naturally occurring, iron storage protein. Ferritin consists of 24-subunits that assemble around an 8 nm core of $Fe_2O_3 \cdot (H_2O)_n$, which can contain up to 4500 iron atoms. The ferritin apo-protein has been used to produce many different types of NPs for multiple potential uses [29, 37, 38].

Other proteins, that do not naturally form NPs, have also been used to template NP synthesis with multiple metal salts. Two of the most prominent of these proteins include human serum albumin (HSA) and bovine serum albumin (BSA) [27, 30, 32–34, 39]. The investigation into the application of these proteins to nucleating NPs is likely due to their relatively low cost and ubiquity in research laboratories. These proteins provide a relatively cheap way to rapidly, and without further functionalization, produce biocompatible NPs. In one example of HSA or BSA nucleating AuNP synthesis, the protein is mixed with $HAuCl_4$ in water and heated. The protein is denatured by the heat and acidity, upon which it is able to reduce and bind to the gold and, further, to encapsulate the growing NP.

All of these examples cite the protein-templated creation of colloidal NPs, which are zero-dimensional (0D) materials. In order to construct more functional materials harboring NPs, the organization of these particles must be controlled in one-dimensional (1D), two-dimensional (2D) or three-dimensional systems. Several design principals from biological organization have been adapted in order to create multidimensional materials that incorporate NPs. One of the most promising examples of this has been the use of DNA to control both the shape and long-range organization of NP-based constructs in solution. Mirkin and co-workers [40] have described several design rules for dictating NP superlattice structure as dictated by individual NP shape and DNA. Unfortunately, these superlattice structures are only stable in solution, as confirmed by small angle x-ray scattering measurements, and are destabilized upon transition to the solid state. DNA, amphiphilic (as utilized by phospholipids and proteins), protein quaternary structure (specifically as found in viruses) and amyloid organizations have been used to template 1D materials containing NPs [5, 6, 8, 9, 14, 17, 18, 24, 41–45]. The basic premise of these schemes is as follows: (i) a material is self-assembled through non-covalent interactions; (ii) the material is designed such that it contains chemical moieties that will bind to NPs on its solvent exposed surface; (iii) a metal salt and reducing agent are added; and (iv) metal NPs form on the surface of the 1D material.

These 1D materials have many potential applications with electronic, magnetic and analytical functions [45]. It is reasonable to compare the materials to wires by sight alone (scanning electron microscopy (SEM), low magnification optical microscopy and by eye), and, many of these materials that were developed with gold or silver NPs have been tested for conductivity properties [8, 9, 14, 17, 18, 24, 41]. The soft nature of the organic substrate combined with the conductive properties of the inorganic NP make these 'wires' attractive

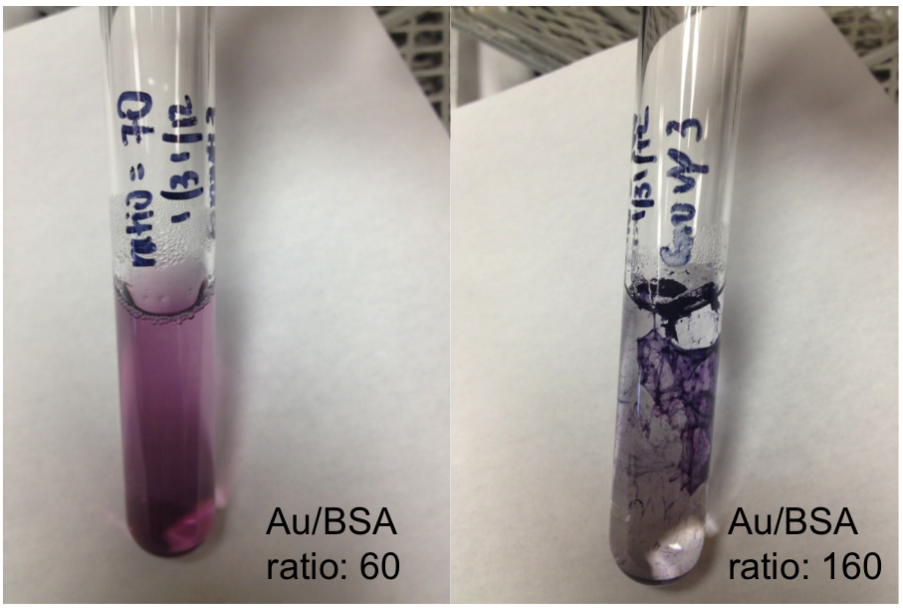

Figure 1. The image on the left shows BSA–AuNPs prepared with a Au/BSA ratio of 60. This produces a purple solution in which the AuNPs are evenly distributed. The image on the right shows BSA–AuNPs prepared with a Au/BSA ratio of 160. This produces purple fibers which are suspended in a clear solution.

for use in flexible electronics. These 1D frameworks could also be the initiation point for building higher-order materials.

In the current paper, we describe a novel and cost effective method for generating 1D protein-NP materials using BSA (a readily available and inexpensive protein) and chloroauric acid in aqueous solution. The 1D fibers form concurrently in solution with 0D gold NPs. As opposed to other studies creating 1D aggregates of NPs, the synthesis we present here is a one-pot setup. The result of this synthesis is a set of fibers, in which the protein and not the AuNPs, are presented at the interface with solution. In some instances (the highest Au/BSA ratios) we observe 2D mesh networks along with the 1D fibers. The 1D and 2D aggregates will be the basis for more complex biomineralization studies, and we believe that they also may be potentially useful for creating functional devices (for instance, detection of unfolded proteins or flexible conductors). The current study, however, focuses solely on determining the solution conditions that lead to formation of AuNPs and 1D fibers and understanding the solution environment after fiber and AuNP formation.

2. Materials and methods

The materials in this paper are produced from a modified, literature-based method for synthesizing protein-capped gold NPs [27]. In order to produce either homogeneous suspensions of BSA–AuNP colloids or BSA–AuNP fibers the following protocol was used: a solution of chloroauric acid (final concentration of 0.25 mM), BSA (at the appropriate concentration) and water was prepared in a test tube and capped; the mixture was heated for 4 h at 80 °C. For spectroscopic analyses, the samples were centrifuged in order to remove any solids prior to characterization. This procedure was performed for multiple Au/BSA ratios from 18 to 160. Further experimental methods, including the specifics about the instrumentation used, can be found in the supplementary information method (available from stacks.iop.org/STAM/14/065004/mmedia).

3. Results and discussion

In our opinion, the most striking observation from this study is that, as the Au/BSA ratio is systematically changed, two different outcomes are produced. At low ratios, colloidal BSA–AuNPs are dispersed in solution. At high ratios, however, a solid, fibrous material containing AuNPs is observed. Figure 1 illustrates the two types of reaction products that we observe. A Au/BSA ratio of 60 produces a homogeneous solution of NPs, evenly distributed throughout the liquid. This results in a solution of purple color, as is seen for other solutions of gold NPs. This result is consistent for Au/BSA ratios between 30 and 120. A Au/BSA ratio of 160 produces purple fibers, which are suspended in a clear solution. It appears that all of the gold NPs are trapped inside of the fibers, as the external solution shows no indication of purple coloring. This result is consistent for Au/BSA ratios between 120 and 160.

As the Au/BSA ratio is varied from 20 to 160, outcomes can be clustered into three main regions. At Au/BSA ratios of 20 and 30, minimal to no NP formation is observed. Between Au/BSA ratios of 40 and 120, homogeneous purple solutions are produced with the higher ratios yielding a more intense purple color. At a Au/BSA ratio of roughly 130, there appears to be a distinct cut-off in which the resultant solution is clear and contains purple fibers. At ratios above 130, the outcome of the synthesis is a clear solution containing purple fibers. This descriptive data is born out in figure S1 (available from) (photo) and figure 2 (UV–Vis data). In all of these cases, the

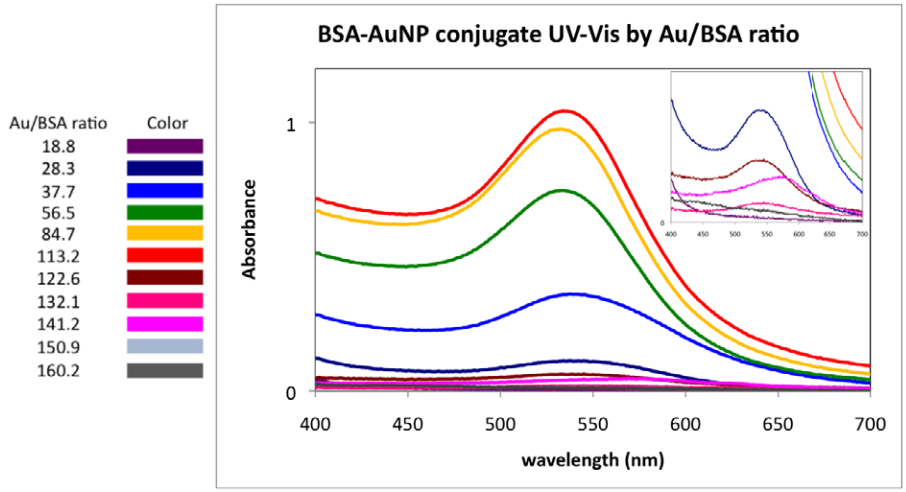

Figure 2. UV–Vis spectra of resulting solutions from BSA–AuNP synthesis taken for different Au/BSA ratios. The key on the left matches the spectrum color to a Au/BSA ratio. The samples were prepared as described in the text (i.e. reaction for 4 h at 80 °C) with an additional centrifugation step (4000 g at room temperature for 10 min) in order to remove any fibers from solution. In these spectra, the absorbance feature near 530 nm indicates NP formation. At the lowest Au/BSA ratio (18.8), there is no observed AuNP formation. As the Au/BSA ratio increases to 113, the intensity of the absorption band near 530 nm also increases. At higher ratios, this band seems to disappear indicating that all of the NPs are trapped in the visible purple fibers.

initial solution pH was between 5.3 and 5.6, and the final solution pH was between 5.0 and 5.3.

To get a better idea of how such different outcomes could be produced, it is instructive to look at how the NPs are produced in the first place. In order to template NP growth, the protein must be able to reduce the Au^{3+} to Au^0 and coordinate to the metal atom. (Either the binding or the reduction could occur first.) BSA contains several sources of reducing electrons. According to the crystal structure for this protein (pdb code: 3V03 [46]), BSA contains 18 disulfide bonds, 2 tryptophan residues and 18 tyrosine residues. (Other potential sources of reducing electrons in the solution are chloride and water.) In order for the gold to access these electrons from the protein, the protein must unfold. The unfolding is facilitated by heating [47] the solution in the acidic environment provided by the chloroauric acid. (When $AuCl_3$ is used instead of $HAuCl_4$, no NPs are produced unless an acid, such as HCl is added. Data not shown.) Reduction of disulfide bonds also destabilizes the folded protein structure in relation to the unfolded protein. The heat and low pH also affect the kinetics and thermodynamics of the redox reactions. There is evidence from similar procedures that AuNPs can be formed in this manner by heating to just 40 °C [27]. Predictably, it requires a much longer time in order to bring the reaction to completion. Temperature plays a role in many of the requirements for this synthesis, influencing the rate at which reactants cross activation barriers, facilitating protein unfolding, and affecting the thermodynamics of the oxidation/reduction reactions. The protein can bind to either Au^{3+} or Au^0. Histidine, cysteine, aspartic acid, glutamic acid and the protein backbone nitrogen and oxygen atoms are all possible ligands for gold coordination. Again, an unfolded protein allows greater access to these binding sites. As the NP grows, it is surrounded by proteins in various unfolded states.

The questions of what brings about fiber formation in the high Au/BSA ratio systems have answers that are not nearly so straightforward. Each NP that is produced is surrounded by one protein or, more likely, multiple proteins. These proteins ensure that the AuNP remains suspended in the aqueous solution. The capping-proteins are either fully or partially unfolded. There are a number of interactions that can drive unfolded proteins to aggregate. Notably, the hydrophobic/hydrophilic interactions that bring about amyloid formation are likely to play a role in the aggregation. As Dobson has shown, amyloid formation is not limited to Aβ, α-synuclein and other proteins involved in misfolding-based diseases [48–50]. Any protein can undergo amyloid-type aggregation. In the results presented here, the unfolded protein caps the NP. The types of residues that are ligands to the NP are most likely to be hydrophilic. This indicates that there may be a good portion of solvent-exposed hydrophobic residues, which could help to induce aggregation. This leads to the following question: why is it that fiber formation and aggregation are observed at lower protein concentrations (i.e. higher Au/BSA ratios—the gold concentration in our experiments is kept constant)? Another possible explanation is that excess gold ions in solution, those that are not involved in NP formation, facilitate coordination-induced aggregation. There is some precedence for this in the literature for peptide-templated NP synthesis [23]. Coordination-induced aggregation and quaternary structure formation is also the basis for some of the research from the Tezcan laboratory [51]. In all likelihood, for our system, the answer is that there is probably a combination of these forces, along with others that we have not mentioned. The remainder of this report focuses on the structure of the fiber, assessing the size of the NPs in solution and determining the gold content in each of the prepared solutions. Future research will study, in more detail, the properties controlling

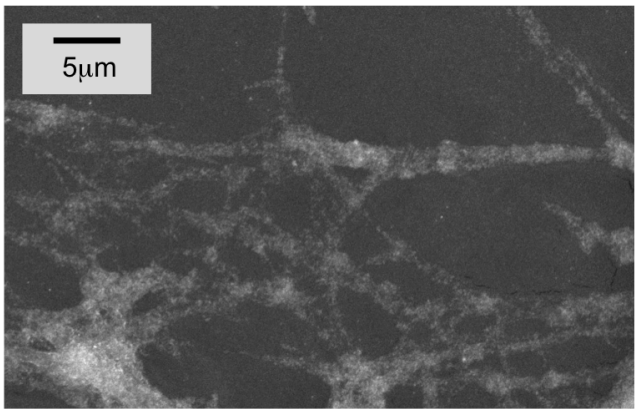

Figure 3. SEM image of several BSA–AuNP fibers. The image displays a grouping of BSA–AuNP fibers of different diameters. The fibers were mounted on carbon tape and sputtered with gold. Some of the fibers seem to interlace. However, these fibers all appear to primarily be of a linear dimension.

fiber formation as well as potential uses for this novel material.

Earlier reports that used similar methods to produce BSA–AuNPs found that the size of the AuNPs, as characterized by transmission electron microscopy (TEM) were roughly 10 nm or smaller in diameter [27, 32–34, 39, 46], and our findings are in line with this assessment. We used electron microscopy to characterize the fibers. An SEM image of these fibers is shown in figure 3. TEM images of the fibers and the suspended NPs are shown in figure 4. There are a few observations of note. First, the TEM images indicate that the NPs are roughly 50 nm in diameter. However, the resolving power of our instrument does not match the instruments used in comparable studies [27, 32–34, 39, 46]. The particles even appear fuzzy or blurred in the images that we have taken. It is more likely that the size is on the order of these previous studies as more closely in line with our dynamic light scattering (DLS) data as shown in figure 5 and table 1. The SEM image of the fibers indicates that they are nearly all linear while displaying some minor amount of branching and overlapping. In the SEM image, these fibers also have different diameters. In the course of our studies, we also observed fibers with a left-handed helical twist (figure S2) (available from stacks.iop.org/STAM/14/065004/mmedia). Unfortunately we do not understand how to control when this structure is or is not formed. The final observation comes from the TEM of the BSA–AuNP fibers. The image shows individual NPs arranged next to one another with little room in between. This observation reinforces our argument that protein–protein, amyloid-type or charge–charge interactions are driving fiber formation. The full width of these fibers (as measured by TEM) is on the order of 400 nm. This is consistent with other TEM images we collected. We are unsure if all of the individual fibers are 400 nm in diameter. If this were the case, the fibers seen at lower magnifications in SEM would have to be aggregates or bundles of multiple fibers.

To further investigate the transition from homogeneous solution of NPs to BSA–AuNP fibers, we employed UV–Vis spectroscopy and DLS to assess any NPs that remain in solution. UV–Vis spectra will indicate two things. Firstly, the presence of purple coloration, which arises from an absorption feature near 530 nm, indicates that there are AuNPs in solution. Secondly, the precise location of this feature can give an indication of the relative size of the NP (this includes the size of the central AuNP core combined with the size of the protein shell that surrounds the core) [52]. A red-shift of this absorption feature corresponds to an increase of the size of the BSA–AuNP in solution. In order to gain a better understanding of the size of BSA–AuNPs in solution, we also used DLS. It should be noted that analysis of DLS data requires the assumption that particles in solution are perfectly spherical. We do not assume that this is the case for the BSA–AuNPs that we have made, especially in the instances where the overall BSA–AuNP size begins to grow. However, the DLS data assists in forming a qualitative understanding of the NPs in solution.

Figure 2 highlights the changes in absorption of the feature at 530 nm. At the lowest Au/BSA ratio (20), there is no detectable absorption feature present at this wavelength. As the Au/BSA ratio increases from this point, the intensity of this absorption band also increases until a Au/BSA ratio of 113.2 is reached. This indicates that BSA–AuNP concentration also increases. At larger ratios, the intensity of this feature decreases significantly and disappears altogether. This decrease correlates to the appearance of purple BSA–AuNP fibers in the reaction mixture. Figure 5 shows the position of the absorbance maxima and the NP diameter (as measured by DLS) as a function of Au/BSA ratio. The trends in these graphs give a qualitative description of what is occurring in solution. At lower Au/BSA the data remain fairly constant. At Au/BSA of below 122.6, the absorbance maximum is steady at around 535 nm. For Au/BSA of below 94, the DLS data indicate an average NP diameter of roughly 20 nm. (If we assume that the gold core of these NPs is roughly 10 nm in diameter, then the remaining 10 nm will consist of a shell of aggregated proteins with a 5 nm diameter.) As the Au/BSA ratio increases, both the absorption maximum and the DLS diameter measurements change to reflect larger particles in solution. The UV–Vis spectra show significant peaks in the absorption feature near 530 nm until the Au/BSA ratio reaches 122.6. This is the ratio where we observe the onset of fiber formation in solution. This absorption feature red shifts to 571 nm at a ratio of 141.2. However, this feature is very low in intensity (see table 1) and may be due to aggregates that are not removed from solution during the centrifugation process. The DLS data indicate that the particles increase in size up to 268 nm at a Au/BSA ratio of 122.6. These data, taken together, qualitatively show that NP size remains fairly constant over the range where BSA–AuNPs create a homogeneous solution. As fiber formation sets in, it appears as though most of the BSA–AuNPs are sequestered into the fiber with very few remaining in solution.

In order to follow the gold in solution, we utilized atomic absorption (AA) spectroscopy. The data are shown in figure 6. These samples, as in the case of the UV–Vis and DLS

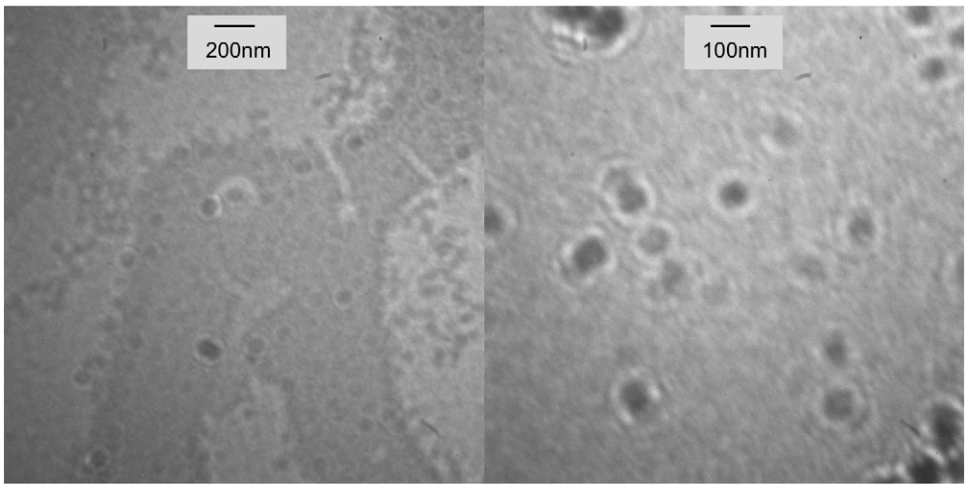

Figure 4. TEM image of a BSA–AuNP fiber (left) and BSA–AuNPs from a homogeneous solution (right) at different magnifications. The image of the fiber shows a material with a width of roughly 400 nm. This image also displays a branching point in the fiber. The image also indicates that the BSA–AuNPs are in close proximity to one another within the fiber.

measurements, were centrifuged in order to remove any fibers from suspension in solution. These data clearly show that, for samples that have homogeneous BSA–AuNPs colloids, there is measurable gold in the solution. As fibers begin to form however, the concentration of gold in solution falls below the detection limit of the instrument. This indicates that most of the gold, whether it is part of a NP or remaining in an ionic state, is trapped within the fibers. The UV–Vis data also backs up this assessment. We have already discussed the disappearance of the absorbance feature near 530 nm in solution for reaction conditions that create fibers, which shows that BSA–AuNPs are confined within the fibers (see figure 2). The UV–Vis spectra also give clues as to the presence of Au^{3+} in solution. Aqueous $AuCl^{4-}$ has a yellow color as evidenced by an absorption feature near 325 nm (see figure S4 (available from stacks.iop.org/STAM/14/065004/mmedia) for a Au/BSA ratio of 18). This feature is noticeably absent for solutions in which fibers are formed. While we cannot accurately describe how much Au^{3+} is converted into gold NPs, we can say that most of the gold is encapsulated within the fibers for reaction conditions that produce BSA–AuNP fibers.

All of these data, taken together, project a possible explanation for how NP synthesis and fiber formation occur. At low Au/BSA ratios, gold NP cores are surrounded by fully or partially unfolded proteins. It is likely that these capping proteins display some hydrophobic residues on its solvent exposed surface. In order to reduce the free energy of the system, other proteins, which are not involved in capping NPs, must interact with these exposed hydrophobic residues. This protein–protein interaction can also be assisted through Au^{3+} and Cl^{-} driven salt-bridge formation. At low Au/BSA ratios there will be free proteins left in solution. As the Au/BSA ratio increases, there are fewer and fewer free proteins in solution. As the Au/BSA ratios near 122, the system has just enough

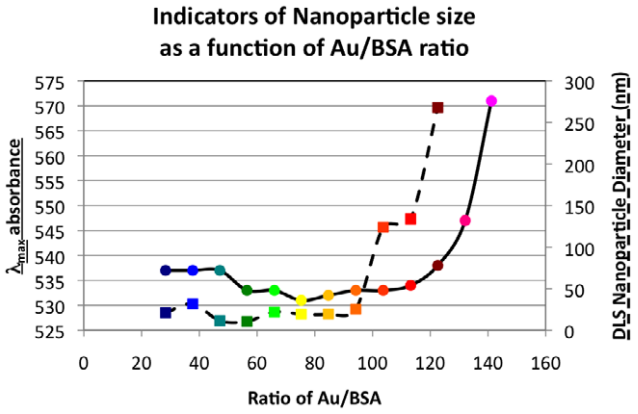

Figure 5. Graph showing the trends in UV–Vis absorption maxima (solid line) and DLS determined NP diameter (dashed line) as a function of Au/BSA ratio. Both curves qualitatively show a single trend: NP size remains relatively constant until a Au/BSA ratio of 94. After this ratio, both the UV–Vis spectra and the DLS data indicate an increase in size. The DLS data cut out for ratios above 122.6 due to a lack of signal from no observed particles in solution. In the UV–Vis spectra, a ratio of 122.6 also shows a substantial decrease in absorbance intensity. Presumably this is also due to a reduced amount of NPs in solution. The reduced signal in both UV–Vis (as shown in figure 2) and DLS corresponds to the appearance of BSA–AuNP fibers in solution.

proteins to cap the growing NP, but not enough to stabilize the system by shielding hydrophobic residues from the aqueous solution. This causes the BSA–AuNPs to aggregate and form fibers. These fibers appear to contain all of the BSA–AuNPs as well as any free $AuCl^{4-}$ in solution. As the Au/BSA ratio increases from 120 to 160 and above, the interaction between capping proteins may become stronger and result in materials with higher-order organization.

Table 1. This table shows the data recorded for UV–Vis peak position along with peak height for the absorption feature near 530 nm. The table also shows the scattering diameter and % deviation as calculated after the DLS measurement.

	UV–Vis γ_{max}		DLS	
Au/BSA ratio	Peak position (nm)	Peak height	Diameter (nm)	Deviation (%)
18.8	No peak	No peak	No peak	No peak
28.3	537	0.112	21.2	9
37.7	537	0.36	31.7	5
47.1	537	0.608	11.5	11
56.5	533	0.746	10.7	11
66	533	0.866	22	7
75.3	531	0.86	19.4	4
84.7	532	0.975	19.5	5
94.2	533	0.956	25.4	7
103.7	533	0.974	124	2
113.2	534	1.043	134	4
122.6	538	0.063	268	12
132.1	547	0.02	No peak	No peak
141.2	571	0.046	No peak	No peak
150.9	No data	No data	No peak	No peak
160.2	No data	No data	No peak	No peak

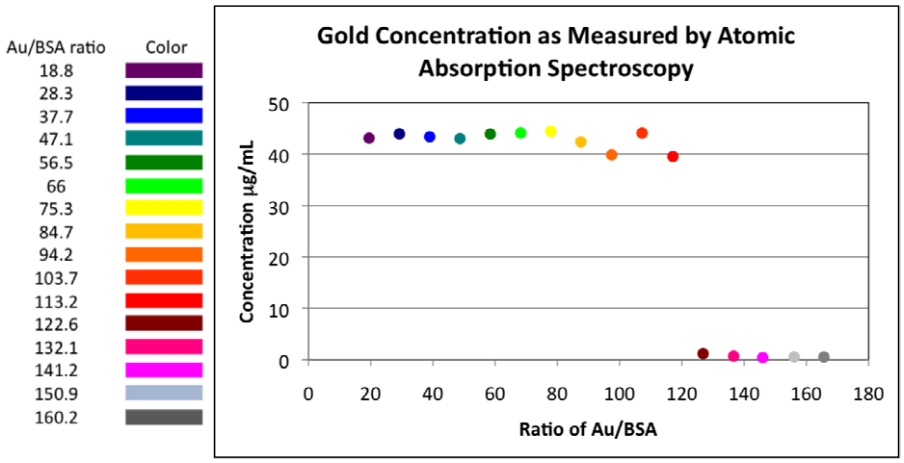

Figure 6. Concentration of gold as measured by AA spectroscopy. The samples were prepared, post BSA–AuNP synthesis, by centrifuging the mixture. The solution was analyzed by AA. The gold concentration stays fairly constant in the region where homogeneous NPs are observed. The concentration of gold begins to drops at a Au/BSA ratio of 122.6, which corresponds to the onset of fiber formation. At higher Au/BSA ratios, where fiber formation is observed, the concentration of gold in solution falls below the instrument detection limit.

4. Conclusions

This paper presents a novel method for carrying out concurrent 0D and 1D biomineralization. The 1D fibers created here encapsulate gold NPs. These fibers are held together by the same forces that drive protein folding or protein aggregation. The fibers are different from other 1D NP assemblies in that the NPs are confined within the fiber and not displayed on the fiber's external surface. Because of this, we expect to be able to design fibers with specific biomolecular sequences. These fibers, then, could be the basis for: amyloid detection devices in which the binding of amyloid proteins causes a change in the AuNP plasmon, or as artificial tissue scaffolds in which the fiber presents specific biochemical signaling sequences. Future work will explore the physical and chemical properties of these novel materials along with exploration into the types of applications (biomedical and commercial) that these materials may be useful for.

Acknowledgments

MRH thanks Jeesoeng Hwang of NIST in Gaithersburg , MD for use of the DLS instrument. MRH also thanks Professor Stefano Costanzi of American University and Professor Mustafa Güler of Bilkent University for their discussions and helpful guidance. We are grateful to the US Air Force Office of Scientific Research for funding and personnel and also to the US Naval Academy for facilities utilized to perform this work. Any opinions, findings and conclusions or recommendations expressed in this material are those of the authors and do not necessarily reflect the views of the US Air Force or the US Navy. The paper was written through

contributions of all authors. All authors approved to the final version of the paper.

References

[1] Ball P 2001 *Nature* **409** 413
[2] Dickerson M B, Sandhage K H and Naik R R 2008 *Chem. Rev.* **108** 4935
[3] Weiner S and Addadi L 1997 *J. Mater. Chem.* **7** 689
[4] Algar W R, Prasuhn D E, Stewart M H, Jennings T L, Blanco-Canosa J B, Dawson P E and Medintz I L 2011 *Bioconjugate Chem.* **22** 825
[5] Choi C L and Alivisatos A P 2010 *Annu. Rev. Phys. Chem.* **61** 369
[6] Gao X Y and Matsui H 2005 *Adv. Mater.* **17** 2037
[7] Lohse S E and Murphy C J 2012 *J. Am. Chem. Soc.* **134** 15607
[8] Nie Z, Petukhova A and Kumacheva E 2010 *Nature Nanotechnol.* **5** 15
[9] Pileni M P 2001 *J. Phys. Chem.* B **105** 3358
[10] Rana S, Yeh Y C and Rotello V M 2010 *Curr. Opin. Chem. Biol.* **14** 828
[11] Carter C J, Ackerson C J and Feldheim D L 2010 *ACS Nano* **4** 3883
[12] Gugliotti L A, Feldheim D L and Eaton B E 2009 *J. Am. Chem. Soc.* **131** 11634
[13] Bakshi M S 2011 *J. Phys. Chem.* C **115** 13947
[14] Kotov N A and Stellacci F 2008 *Adv. Mater.* **20** 4221
[15] Cole K E and Valentine A M 2007 *Biomacromolecules* **8** 1641
[16] Acar H, Genc R, Urel M, Erkal T S, Dana A and Guler M O 2012 *Langmuir* **28** 16347
[17] Chen C-L and Rosi N L 2010 *Angew. Chem. Int. Edn Engl.* **49** 1924
[18] Chen C-L, Zhang P and Rosi N L 2008 *J. Am. Chem. Soc.* **130** 13555
[19] Chiu C Y, Li Y J, Ruan L Y, Ye X C, Murray C B and Huang Y 2011 *Nature Chem.* **3** 393
[20] Coppage R, Slocik J M, Briggs B D, Frenkel A I, Heinz H, Naik R R and Knecht M R 2011 *J. Am. Chem. Soc.* **133** 12346
[21] Coppage R, Slocik J M, Briggs B D, Frenkel A I, Naik R R and Knecht M R 2012 *ACS Nano* **6** 1625
[22] Slocik J M, Stone M O and Naik R R 2005 *Small* **1** 1048
[23] Tan Y N, Lee J Y and Wang D I C 2010 *J. Am. Chem. Soc.* **132** 5677
[24] Whaley S R, English D S, Hu E L, Barbara P F and Belcher A M 2000 *Nature* **405** 665
[25] Khalily M A, Ustahuseyin O, Garifullin R, Genc R and Guler M O 2012 *Chem. Commun.* **48** 11358
[26] Bakshi M S, Kaur H, Banipal T S, Singh N and Kaur G 2010 *Langmuir* **26** 13535
[27] Bakshi M S, Kaur H, Khullar P, Banipal T S, Kaur G and Singh N 2011 *J. Phys. Chem.* C **115** 2982
[28] Burt J L, Gutierrez-Wing C, Miki-Yoshida M and Jose-Yacaman M 2004 *Langmuir* **20** 11778
[29] Butts C A, Swift J, Kang S G, Di Costanzo L, Christianson D W, Saven J G and Dmochowski I J 2008 *Biochemistry* **47** 12729
[30] Canaveras F, Madueno R, Sevilla J M, Blazquez M and Pineda T 2012 *J. Phys. Chem.* C **116** 10430
[31] Dedeo M T, Finley D T and Francis M B 2011 *Molecular Assembly in Natural and Engineered Systems* 103 ed S Howorka (New York: Academic) p 353
[32] Khullar P, Singh V, Mahal A, Dave P N, Thakur S, Kaur G, Singh J, Kamboj S S and Bakshi M S 2012 *J. Phys. Chem.* C **116** 8834
[33] Liu L, Zheng H Z, Zhang Z J, Huang Y M, Chen S M and Hu Y F 2008 *Spectrochim. Acta* A **69** 701
[34] Sen T, Haldar K K and Patra A 2008 *J. Phys. Chem.* C **112** 17945
[35] Slocik J M and Wright D W 2003 *Biomacromolecules* **4** 1135
[36] Witus L S and Francis M B 2011 *Account. Chem. Res.* **44** 774
[37] Uchida M, Klem M T, Allen M, Suci P, Flenniken M, Gillitzer E, Varpness Z, Liepold L O, Young M and Douglas T 2007 *Adv. Mater.* **19** 1025
[38] Amos F F, Cole K E, Meserole R L, Gaffney J P and Valentine A M 2013 *J. Biol. Inorg. Chem.* **18** 145
[39] Focsan M, Gabudean A M, Canpean V, Maniu D and Astilean S 2011 *Mater. Chem. Phys.* **129** 939
[40] Macfarlane R J, Lee B, Jones M R, Harris N, Schatz G C and Mirkin C A 2011 *Science* **334** 204
[41] Chang W-S, Slaughter L S, Khanal B P, Manna P, Zubarev E R and Link S 2009 *Nano Lett.* **9** 1152
[42] Hwang L, Chen C L and Rosi N L 2011 *Chem. Commun.* **47** 185
[43] Hwang L, Zhao G P, Zhang P J and Rosi N L 2011 *Small* **7** 1939
[44] Li L S and Stupp S I 2005 *Angew. Chem., Int. Edn Engl.* **44** 1833
[45] Tang Z Y and Kotov N A 2005 *Adv. Mater.* **17** 951
[46] Majorek K A, Porebski P J, Dayal A, Zimmerman M D, Jablonska K, Stewart A J, Chruszcz M and Minor W 2012 *Mol. Immunol.* **52** 174
[47] Murayama K and Tomida M 2004 *Biochemistry* **43** 11526
[48] Baldwin A J *et al* 2011 *J. Am. Chem. Soc.* **133** 14160
[49] Chiti F and Dobson C M 2006 *Annu. Rev. Biochem.* **75** 333
[50] Dobson C M 2003 *Nature* **426** 884
[51] Brodin J D, Ambroggio X I, Tang C Y, Parent K N, Baker T S and Tezcan F A 2012 *Nature Chem.* **4** 375
[52] Pesika N S, Stebe K J and Searson P C 2003 *J. Phys. Chem.* B **107** 10412